

overlap because of the zig-zag boundaries. The overlapping leads to annihilation of the thinner black reversed areas. Such annihilation might then explain why only two black reversed areas are observed. The inset in Fig. 1B shows a gradual transition, indicating a structure dominated by grains. Owing to the reduced crystallinity of Co II, zig-zag walls are not formed. Correspondingly, a stable reversed area is seen much closer to the center of the structure.

We note that the radii of the experimentally observed inner rings are not exactly reproduced by the calculations. For example, in Co I the second reversal back to the original direction occurs at smaller field values than expected and the subsequent third and fourth reversals even more so. The same phenomenon is observed in Co II. The details of the inner structure of the patterns cannot be calculated with the simple LL approach unless one assumes that some of the material properties vary with time. Supposing that intrinsic properties such as M_S and H_A are constant, one is forced to assume that α is time dependent. Two different mechanisms might lead to a time-dependent effective damping constant α_{eff} . The first one is the excitation of magnons. The field pulses are built with frequencies close to the frequency band of magnons, hence magnon excitation might be enhanced. This can lead to an increase in energy dissipation and thus to an increase in α_{eff} . The other mechanism is electron-electron scattering (11). If \vec{M} precesses at a different rate in each location, this scattering will be very strong, again leading to a larger effective damping constant.

Ultimately, direct observation of \vec{M} during the precessional motion is desired. Freeman and co-workers (12) have shown that this is indeed possible with the magneto-optic Kerr effect using picosecond laser pulses. Other groups use inductive probing (13) or spin-polarized tunneling (14). Another exciting prospect comes from the development of the Next Linear Collider (15, 16). In this project, microstructured electron pulses will be developed that deliver a train of very strong magnetic field pulses of picosecond length, ideal for observing the dynamics of the reversal.

These results have implications for longitudinal magnetic recording and demonstrate the possibility of recording at extremely high data rates if problems arising from transitions between regions of oppositely magnetized material can be overcome. This requires a magnetic medium consisting of either identical grains or single-domain particles (17).

References and Notes

1. M. Ledermann, S. Schultz, M. Ozaki, *Phys. Rev. Lett.* **73**, 1986 (1994).
 2. W. Wernsdorfer et al., *ibid.* **78**, 1791 (1997).

3. S. Y. Chou, P. R. Krauss, L. Kong, *J. Appl. Phys.* **79**, 6101 (1996).
 4. C. H. Back et al., *Phys. Rev. Lett.* **81**, 3251 (1998).
 5. H. C. Siegmann et al., *J. Magn. Magn. Mat.* **151**, L8 (1995).
 6. A. Lyberatos and R. W. Chantrell, *J. Phys. Condens. Matter* **9**, 2623 (1997).
 7. W. D. Doyle, S. Stinnet, C. Dawson, L. He, *J. Magn. Soc. Jpn.* **22**, 91 (1998).
 8. R. Allenspach, *J. Magn. Magn. Mat.* **129**, 160 (1994).
 9. Values for the spin-lattice relaxation time are found to lie in the realm of 100 ps. A. Vaterlaus, T. Beutler, D. Guarisco, M. Lutz, F. Meier, *Phys. Rev. B* **46**, 5280 (1992); A. Scholl, L. Baumgarten, R. Jacquemin, W. Eberhard, *Phys. Rev. Lett.* **79**, 5146 (1997), and references therein.
 10. α is in fact very sensitive to the quality of the sample. It is known that only high-quality samples show small damping constants. Also, the value of α might be different from values determined in ferromagnetic resonance (FMR) experiments. In FMR, a small stationary radio frequency excitation causes coherent precession around the effective field. In our experiments, in contrast, the excitation is strong and nonstationary.
 11. D. Oberli, R. Burgermeister, S. Riesen, W. Weber, H. C. Siegmann, *Phys. Rev. Lett.* **81**, 4228 (1998).
 12. W. K. Hiebert, A. Stankiewicz, M. R. Freeman, *ibid.* **79**, 1134 (1998).
 13. T. J. Silva, T. M. Crawford, C. T. Rogers, *J. Appl. Phys.* **85**, 7849 (1999).
 14. R. H. Koch et al., *Phys. Rev. Lett.* **81**, 4512 (1998).
 15. T. Nakanishi, in *Proceedings of LE '98*, St. Petersburg, Russia, 2 to 5 September 1998 (SPES-Lab-Publishing, St. Petersburg, Russia, 1998).
 16. C. Adolphson et al., "Zeroth-Order Design Report for the Next Linear Collider," Stanford Linear Accelerator Center (Stanford Univ., Stanford, CA 1996).
 17. C. Stamm et al., *Science* **282**, 449 (1998).
 18. We gratefully acknowledge the valuable input of several people at the Final Focus Test Beam facility and Physical Electronics Laboratory, and the assistance of D. Guarisco with some of the programming. C.H.B. thanks the Swiss National Fund for financial support. This work was supported in part by the U.S. Department of Energy under contract no. DE-AC03-76SF00515.

11 January 1999; accepted 22 June 1999

Current-Induced Switching of Domains in Magnetic Multilayer Devices

E. B. Myers,¹ D. C. Ralph,^{1*} J. A. Katine,² R. N. Louie,² R. A. Buhrman²

Current-induced switching in the orientation of magnetic moments is observed in cobalt/copper/cobalt sandwich structures, for currents flowing perpendicularly through the layers. Magnetic domains in adjacent cobalt layers can be manipulated controllably between stable parallel and antiparallel configurations by applying current pulses of the appropriate sign. The observations are in accord with predictions that a spin-polarized current exerts a torque at the interface between a magnetic and nonmagnetic metal, due to local exchange interactions between conduction electrons and the magnetic moments.

Devices containing alternating nanometer-scale-thick layers of ferromagnetic and nonmagnetic metals exhibit giant magnetoresistance (GMR), because current flow is strongly affected by the relative orientation of the magnetic moments in the layers (1). Specifically, antiparallel alignment of the moments gives a higher electrical resistance than parallel alignment. According to Newton's Third Law, one might also expect an inverse effect; that is, electrons scattering within the device may affect the moments in the magnets. Recent calculations indicate that spin-polarized currents flowing perpendicularly through magnetic multilayers may transfer angular momentum between layers, thereby imparting a torque on the magnetic moments (2-5). Experiments have found evidence of current-

induced changes in the resistance of Cu/Co multilayers (6, 7) and granular alloys (6), nickel nanowires (8), and manganite junctions (9), but the nature of the excitations has not been clear. We report experimental studies using a Co/Cu/Co sandwich structure and verify the prediction of (2), that an applied current can be used to controllably switch magnetic domains between different orientations. As predicted by the spin-transfer theory (2), there is an asymmetry as a function of the direction of current bias, so that domains in the two magnetic layers can be aligned antiparallel by currents flowing in one direction, and then reoriented parallel by reversing the current flow. This effect provides a mechanism for a current-controlled magnetic memory element.

We employ a sample geometry suggested by Slonczewski (Fig. 1A) (5), a metal point contact adjacent to two Co layers separated by a Cu spacer. One Co layer (layer 1) is thin (≤ 10 nm) and the other (layer 2) much thicker (100 nm), with the aim that intralayer exchange forces will make the magnetic mo-

¹Laboratory of Atomic and Solid State Physics, Cornell University, Ithaca, NY 14853, USA. ²School of Applied and Engineering Physics, Cornell University, Ithaca, NY 14853, USA.

*To whom correspondence should be addressed. E-mail: ralph@msc.cornell.edu

ments in the thicker layer less easily reoriented by a current-induced torque. The device is made by first using electron-beam lithography and reactive ion etching to produce a bowl-shaped hole in an insulating silicon nitride membrane, with an opening 5 to 10 nm in diameter (I_0). A thick film of Cu is evaporated (base pressure 6×10^{-6} torr) onto the bowl-shaped side of the device to fill the hole and form an interface near the lower edge of the membrane. Without breaking vacuum, layers are then deposited on the opposite side of the device in the sequence: thin Co layer (thickness varied as discussed below), 4 nm Cu, 100 nm Co, 50 nm Cu. No qualitative differences in results were observed for depositions at 77 K and room temperature. Measurements of resistivity on test samples indicate that 2 nm of Co deposited on Si_3N_4 at room temperature does not yet form a fully continuous film, but layers ≥ 4 nm thick are continuous. The 4-nm Cu spacer is sufficiently thick so that there is little exchange coupling between the magnetic layers (I). The differential resistance is measured using a lock-in amplifier. We use the convention that positive bias corresponds to electrons flowing from the Cu electrode into the multilayer.

In (2–5), the torques due to spin transfer are calculated by applying angular momentum conservation during the scattering of partially spin-polarized electron currents from magnetic interfaces. The torques on magnetic layers 1 and 2 are predicted to have the symmetries

$$\tau_{1,2} \propto I \hat{s}_{1,2} \times (\hat{s}_1 \times \hat{s}_2) \quad (1)$$

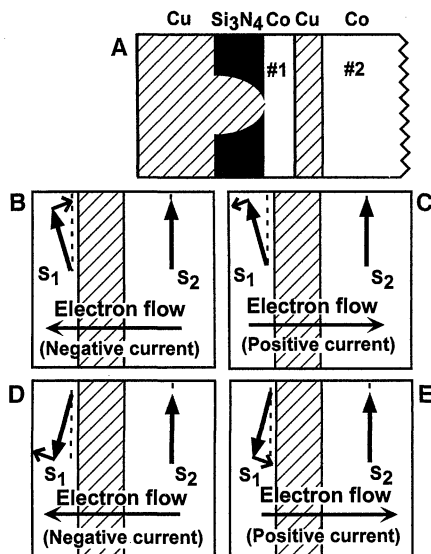


Fig. 1. (A) Cross-sectional device schematic, showing layer #1 and #2. (B through E) Directions of torque on the magnetic moments in layer 1, due to spin transfer by current flow. Parallel alignment of the moments in the two layers is unstable for sufficiently large positive currents, whereas antiparallel alignment is unstable for large negative currents.

where I is the current and \hat{s}_1 and \hat{s}_2 are unit vectors in the direction of the local magnetic moments of each magnetic layer. From this follows an asymmetry with respect to the direction of current. Consider a stability analysis for a small deviation from parallel alignment between \hat{s}_1 and \hat{s}_2 , with \hat{s}_2 assumed fixed, and with a (negative) current applied such that electrons travel from layer 2 to layer 1 (Fig. 1B). The direction of the torque is to turn \hat{s}_1 toward \hat{s}_2 , so the parallel configuration is stable. However, if the current is reversed, the spin-transfer torque is also reversed so as to turn \hat{s}_1 away from \hat{s}_2 (Fig. 1C). For sufficiently large positive currents, this torque may overcome damping and anisotropy effects, making the parallel configuration unstable and leading to dynamical precession or switching. If the magnetic moments of the two layers are originally oriented close to antiparallel, it is the negative bias which pro-

duces an instability, and the positive bias is stable (Fig. 1, D and E).

Figure 2, A through D, shows the differential resistance as a function of current bias at a temperature of 4.2 K for devices with a sequence of deposited thicknesses for the thin Co layer (layer 1). For the thickest layer in the sequence (10 nm) in an applied magnetic field H greater than the saturation field required to align the moments in the layers at zero current bias, the data are very similar to that reported by Tsoi *et al.* (7). For both signs of bias, there is an overall increase in dV/dI at larger currents, which is a familiar effect in metal point contacts due to electron scattering by emission of phonons and magnons (11). In addition, for positive bias, there is a peak in dV/dI , which is not present at negative bias, indicating some form of current-induced change in the resistance of the sample. The peak in dV/dI corresponds to a rounded step

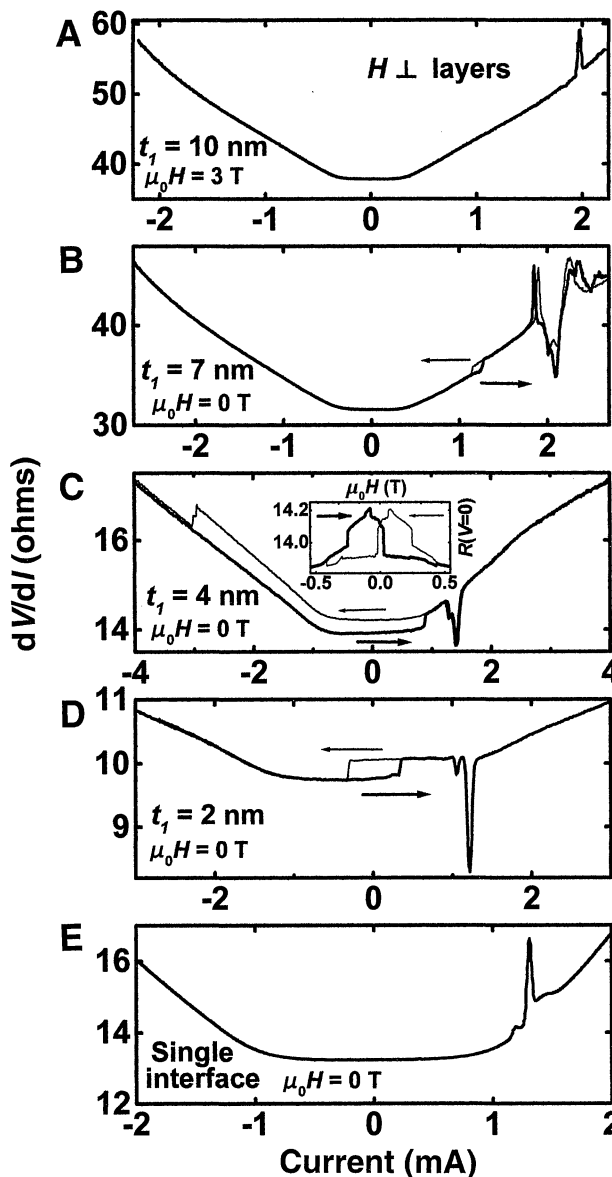


Fig. 2. (A through D) Differential resistance versus current at 4.2 K for Co/Cu/Co sandwich devices in which the deposited thickness t_1 of the thinner Co layer is varied as listed. For samples with a Co layer 4 nm thick and thinner, the hysteresis as a function of current indicates that a magnetic domain in the thin Co layer is flipped controllably between parallel and antiparallel orientations with respect to the thicker Co layer (12). [Inset in (C)] Resistance changes associated with sweeping an in-plane magnetic field about the hysteresis loop. The sweep directions are not mislabeled—samples showing the current-induced switching effect can have maxima in resistance versus increasing H curves at either positive or negative field. This is not surprising, since dipolar forces can force the reversal of some fraction of the domains in a thin-film sample before the sign of the applied field is reversed. (E) Nonhysteretic changes in resistance are present at large positive biases even for a single interface between Cu and Co electrodes.

up in the dc resistance with increasing bias, a step which is continuous and reversible in the sense that the resistance follows the ac modulation of the lock-in amplifier. The asymmetry in current has the sign expected for the spin-transfer-induced instability in the orientation of the magnetic moment in the thin Co layer (2–5). In contrast, if such changes originated from the circumferential self-field generated by the current, one would expect the high-field signals to exist either for both signs of bias or for the opposite sign of bias in some samples, which we do not observe.

Thinner Co layers at $H = 0$ exhibit qualitatively different behavior, which makes clear the nature of the current-induced excitations and the connection to the spin-transfer model (Fig. 2, B through D) (12). For a 7-nm Co layer, the first resistance anomaly at positive bias no longer has the form of a peak in dV/dI (a rounded, continuous step in the dc resistance), but is instead an abrupt hysteretic step in the resistance (9). For even thinner deposited layers, the sample can be switched between two resistance states which are both stable at zero bias. We explain this behavior within the spin-transfer picture by arguing that a large positive current bias (I_{c+}) destabilizes the parallel orientation of the magnetic moments in the two layers near the point contact and switches a particle or domain in the thin Co layer to have magnetization reversed with respect to the moment in the thick Co layer, thus changing the resistance.

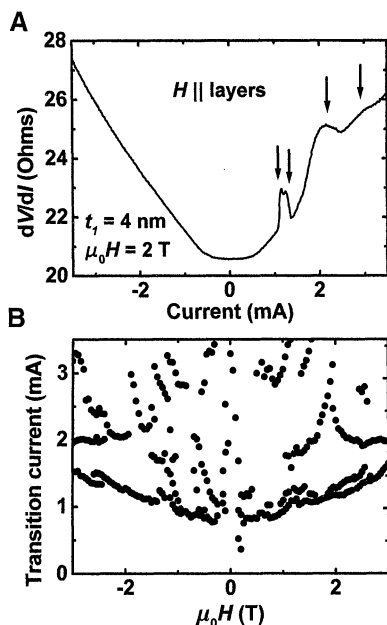


Fig. 3. (A) Curve of dV/dI versus current at 4.2 K with $\mu_0 H = 2$ T parallel to the layers, for a sample with a Co layer (layer 1) 4 nm thick. Multiple features in dV/dI can be observed at large positive bias, indicated by arrows. (B) Dependence on magnetic field for the critical current values of these features.

A sufficiently thin layer is necessary for the stability of such a structure at zero bias; for thick layers, intralayer coupling will force the domain to its original orientation as the current is reduced. Sweeping to sufficiently large negative bias (I_{c-}) destabilizes this reversed domain, as predicted by spin transfer, and returns the magnetic moments to a parallel alignment. The resistance changes associated with the transitions are consistent with this picture, as the states associated with antiparallel alignment of the moments do indeed have higher resistances. The difference in resistance is not large, 3 to 5%. However, this is to be expected for magnetic multilayers near a point contact, simply due to geometry. Consider an electron injected from the Cu electrode through the point-contact orifice. The electron paths which contribute to the difference in resistance for parallel versus antiparallel magnetic orientations are those which are transmitted through the magnetic layers in the parallel configuration but are reflected from layer 2 for antiparallel layers in the precise direction so that they scatter back through the point-contact orifice to reduce the transmitted current. Because the orifice subtends a small solid angle when viewed from the interface of layer 2, the size of the magnetoresistance is reduced by a factor of 2 to 10 (depending on point-contact radius) relative to conventional pillar geometries (13, 14). The changes in resistance associated with the current-induced domain switching are consistent with domain switching caused by sweeping an applied magnetic field about the hysteresis loop near zero current (for example, inset to Fig. 2C).

The current-induced bistable switching is eliminated for H greater than the saturation field needed to force the moments of the two layers into parallel alignment when there is zero current. The switching is also absent for measurements at room temperature in our Co/Cu/Co devices. For either large fields or high temperatures, the data display nonhysteretic features similar to Fig. 3A. We observed the bistable switching at room temperature in one device containing the layers permalloy (4 nm)/Cu (4 nm)/Co (100 nm). This shows that the absence of stable hysteresis at room temperature in most devices is not fundamental, but indicates simply that our reversed domains are small enough to be unstable to thermal fluctuations in the presence of intralayer exchange and dipolar coupling. Higher operating temperatures (and also lower switching currents) might be achieved reproducibly in a geometry where the thin magnetic layer is not part of a continuous film, but is instead an isolated island larger than the superparamagnetic limit but still small enough to have a single magnetic domain (2, 9).

In addition to the hysteretic features at

relatively low bias levels, there are more resistance anomalies in all the samples at larger positive biases. For samples with sufficiently thin magnetic layers and for small applied magnetic fields, such that the resistance shows hysteresis as a function of current bias, the high-bias features are generally dips in dV/dI , corresponding to downward steps in the dc resistance. For thicker layers or larger applied fields, or both, such as to eliminate the hysteresis in current, different high-bias features are present that are generally peaks in dV/dI (7). Similar high-bias features are also present in point contacts which possess only a single interface between thick Cu and Co electrodes (Fig. 2E). Although we do not have a complete microscopic understanding of these features, their presence in samples containing only a single Cu/Co interface suggests that they may be associated with a breakdown in the assumption that the moments in the thicker Co layer remain fixed as a function of bias current. The magnitude of the current density in this high-bias range is greater than 10^9 A/cm², which is sufficient according to estimates of Bazaliy *et al.* (4) to excite spin-wave instabilities within a magnet. The difference in sign (dips or peaks in dV/dI) between the low- and high-field regimes may be a consequence of a difference in the relative orientation of the domains in the two magnetic layers. In the low-field case, as a function of increasing current, we propose that the spin-transfer effect first anti-aligns the moments of two magnetic layers in the point-contact region, and then higher current levels produce excitations of moments within the layers, which lower the resistance because they give deviations from antiparallel alignment. In the high-field regime, the high-bias features likely correspond to increasing deviations from parallel alignment, leading to increases in resistance.

The spin-transfer model leads to a prediction that, for fields greater than the saturation field, the critical current for the first current-induced instability in our geometry should depend linearly on the magnitude of an applied magnetic field [(5), after converting to SI units]

$$I_{\text{crit}} = \frac{e t_1}{\hbar \varepsilon} [23A + 6.3r^2 \alpha_G M_S \mu_0 H_{\text{eff}}] \quad (2)$$

where t_1 is the thickness of the thinner Co film, $\varepsilon \approx 0.7$ is a spin-polarization efficiency parameter which reflects that electrons in Co are not fully spin-polarized, $A \approx 1 \times 10^{-11}$ J/m is the exchange stiffness for Co, r is the point-contact radius, α_G is the Gilbert damping parameter for magnetic excitations, $M_S = 1.45 \times 10^6$ A/m is the Co saturation magnetization, and H_{eff} is a sum of the effective-field contributions from anisotropy, interlayer exchange, and the applied field. Our measurements indicate that the first

instability in the resistance, which we have associated with excitation of the thin-layer moment relative to the thick-layer moment, does have an approximately linear dependence versus H for H greater than the saturation field, although on a fine scale, there are deviations not observed in previous studies (Fig. 3) (7, 9). Subsequent transitions at higher bias, which we have associated with magnetic excitations within the Co layers, show more complicated behavior. The measured zero-field intercepts of I_{crit} for the first transition are generally a factor of 2 to 4 lower than those derived from Eq. 2. We consider this satisfactory agreement, since the layers undoubtedly have nonuniform thickness. The observed slopes of I_{crit} versus H also agree with Eq. 2, provided that we assume a value for the phenomenological damping parameter $\alpha_G = 0.05$ to 0.2 , which is unusually large compared to more macroscopic samples (5). However, we are in a new regime, and there may be large contributions to damping near normal/ferromagnetic interfaces (3) and from intralayer processes for nanometer-scale domains.

Our results have both good and bad implications for applications. The bad news is that the existence of magnetic switching caused by spin transfer places a limit on the current (and therefore the signal levels) that can be used for measuring GMR devices. The good news is that the spin-switching effect may enable magnetic random-access memories in which the memory elements are controlled by local exchange-effect forces rather than by long-range magnetic fields. Slonczewski predicts that the spin-transfer torques should dominate over the effects of the self-magnetic fields from flowing currents for devices up to about 100 nm in diameter (2), so that the point-contact geometry, with its intrinsically low GMR values, should not be necessary to employ the effect.

References and Notes

- For reviews of the science and applications of GMR materials, see the collection of articles in *IBM J. Res. Dev.* **42**, (January 1998). (available electronically at www.research.ibm.com/journal/rd42-1.html)
- J. Slonczewski, *J. Magn. Magn. Mater.* **159**, L1 (1996).
- L. Berger, *Phys. Rev. B* **54**, 9353 (1996).
- Ya. B. Bazaliy, B. A. Jones, S.-C. Zhang, *ibid.* **57**, R3213 (1998).
- J. Slonczewski, *J. Magn. Magn. Mater.* **195**, L261 (1999).
- R. N. Louie, thesis, Cornell University, Ithaca, NY (1997).
- M. Tsoi *et al.*, *Phys. Rev. Lett.* **80**, 4281 (1998); erratum, *ibid.* **81**, 493 (1998).
- J.-E. Wegrowe *et al.*, *Europhys. Lett.* **45**, 626 (1999).
- J. Z. Sun, *J. Magn. Magn. Mater.* **202**, 157 (1999).
- K. S. Ralls, R. A. Buhrman, R. C. Tiberio, *Appl. Phys. Lett.* **55**, 2459 (1989).
- A. G. M. Jansen, A. P. van Gelder, P. Wyder, *J. Phys. C* **13**, 6073 (1980).
- Fig. 2, B through E, exhibits samples never exposed to a magnetic field, but there are no qualitative differences as a function of magnetic history, as long as $H = 0$.
- For a review, see M. A. M. Gijs and G. E. W. Bauer, *Adv. Phys.* **46**, 285 (1997).
- Point-contact measurements of Cu/Co multilayers have previously shown small GMR values; see (6) and M. V. Tsoi, A. G. M. Jansen, J. Bass, *J. Appl. Phys.* **81**, 5530 (1997).
- We thank J. Slonczewski, S. Guéron, and R. H. Silsbee for discussions. The work was supported by the NSF Materials Research Science and Engineering Centers program (DMR-9632275), the Sloan and Packard Foundations, the Office of Naval Research (N00014-97-1-0745), and Defense Advanced Research Projects Agency, and was performed in part at the Cornell node of the National Nanofabrication Users Network, supported by the NSF. E.B.M. was supported by a U.S. Department of Education grant.

15 April 1999; accepted 22 June 1999

Galileo Imaging of Atmospheric Emissions from Io

P. E. Geissler,^{1*} A. S. McEwen,¹ W. Ip,² M. J. S. Belton,³
T. V. Johnson,⁴ W. H. Smyth,⁵ A. P. Ingersoll⁶

The Galileo spacecraft has detected diffuse optical emissions from Io in high-resolution images acquired while the satellite was eclipsed by Jupiter. Three distinct components make up Io's visible emissions. Bright blue glows of more than 300 kilorayleighs emanate from volcanic plumes, probably due to electron impact on molecular sulfur dioxide. Weaker red emissions, possibly due to atomic oxygen, are seen along the limbs, brighter on the pole closest to the plasma torus. A faint green glow appears concentrated on the night side of Io, possibly produced by atomic sodium. Io's disk-averaged emission diminishes with time after entering eclipse, whereas the localized blue glows brighten instead.

Previous spacecraft and ground-based observations have yielded several indications of a tenuous atmosphere on Io. Dominated by SO_2 and its dissociation products SO, O, and S, Io's atmosphere has been studied at wavelengths ranging from the microwave to the ultraviolet (UV) (1, 2). Atomic O, S, Na, and K have been detected in extended neutral clouds escaping from the satellite (3), and recent Hubble Space Telescope (HST) observations of Io have imaged intense auroral emissions at far-UV wavelengths (4). Visible emissions from Io during eclipse by Jupiter were seen by Voyager 1 (5) and suggested to be due to molecular SO_2 (6). HST (7) and ground-based (8, 9) eclipse observations have detected neutral O and Na emissions from Io at visible wavelengths.

The Galileo spacecraft, in orbit around Jupiter since December 1995, can observe optical emissions from Io at a higher spatial resolution than previously possible and from a variety of perspectives unattainable from Earth (10). Diffuse emissions from Io have been seen in 16 distinct solid state imager (SSI) observations acquired during 14 eclipses over the course of

10 orbits. Recorded partly to monitor thermal emission from discrete volcanic centers (11), these observations provide a detailed look at visible aurorae on a solar system satellite. The bulk of the data was acquired with the SSI clear filter, which covers wavelengths between 380 and 1040 nm (12). Two sequences included visible color imaging using the SSI violet (380 to 445 nm), green (510 to 605 nm), and red (615 to 710 nm) filters. Diffuse emissions from Io have not been detected in any of the longer wavelength infrared SSI filters. Here, we describe the morphology of the optical emissions from Io, estimate their brightnesses and radiated powers, and suggest possible interpretations.

The most complete set of eclipse images was acquired on 31 May 1998 during the first of two eclipses in orbit E15 (13) (Table 1). These pictures were centered near a longitude of 70°W , on the orbital leading hemisphere of Io that is also the location of the plasma wake. One set of color images in the violet, green, red, and $1\text{-}\mu\text{m}$ (935 to 1090 nm) filters was taken along with two clear-filter pictures comparing Io's appearance 11 min after the start of the eclipse with its appearance 42 min later. The clear-filter images showed diffuse atmospheric emissions as well as discrete volcanic hot spots on Io's leading hemisphere, whereas only the hot spots were visible in the $1\text{-}\mu\text{m}$ filter. Diffuse emissions with three distinct distributions were seen in the visible color frames (Figs. 1 and 2A). The brightest emissions were blue glows close to the equator near the sub- and anti-Jupiter points, extending several hundred kilometers above the limb. They were seen at red, green, and violet wavelengths but were

¹Lunar and Planetary Laboratory, University of Arizona, Tucson, AZ 85711, USA. ²Institute of Astronomy, National Central University, Chung-Li, Taiwan 320, Republic of China. ³National Optical Astronomy Observatories, Tucson, AZ 85719, USA. ⁴Jet Propulsion Laboratory, MS 23-201B, 4800 Oak Grove Drive, Pasadena, CA 91109, USA. ⁵Atmospheric and Environmental Research, 840 Memorial Drive, Cambridge, MA 02139, USA. ⁶Division of Geology and Planetary Sciences, California Institute of Technology, Pasadena, CA 91125, USA.

*To whom correspondence should be addressed. E-mail: geissler@lpl.arizona.edu